Jurnal Teknologi

Application of Optical Tomography for Monitoring Gas Bubbles Flow Based on Independent Component Analysis Algorithm

Mohd Taufiq Mohd Khairi, Sallehuddin Ibrahim*, Mohd Amri Md Yunus, Mahdi Faramarzi[a], Nor Muzakkir Nor Ayub

Control and Mechatronics Engineering Department, Universiti Teknologi Malaysia, 81310 UTM Johor Bahru, Johor, Malaysia

*Corresponding author: salleh@fke.utm.my

Graphical abstract
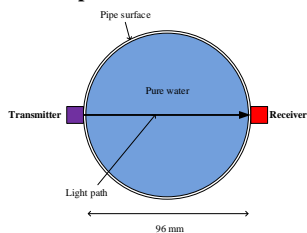
Abstract

This paper presents the monitoring process of gas bubbles flow in water using an optical tomography system. The system is aided by an Independent Component Analysis (ICA) algorithm for distinguishing the gas bubbles in pure water. The optical attenuation model is implemented for studying the light transmissions to different media which is water and air. Several quantities of air are inserted using an air pump which is installed at the bottom of a flow pipe in order to produce the gas bubbles flow upwards. The quantity of air is controlled by using a valve and five types of bubble flow are investigated; a single bubble flow, double bubble's flow, 25% of air opening, 50% of air opening and 100% of air opening. The concentration profiles of the gas bubble flow are constructed. The concentration profile obtained from the experiments shows that the ICA algorithm can be used as a tool for imaging the two-phase flow phase distribution.

Keywords: Optical tomography; fan beam projection; turbidity level; Independent component analysis

1.0 INTRODUCTION

Investigation on two-phase flow measurement involved varying phase distribution and the velocity profile with temporal and spatial coordinates [1]. It is vital to acquire information about the flow behaviour in order to optimise the process and minimise the cost of designing conveying equipment. The identification of spatial distribution of two-phase flow is widely used in large-scale applications such as oil and nuclear industry to provide a better understanding of the flow process [2]. Two-phase flow can be liquid-gas, gas-solid and solid-liquid. Investigation on gas bubble behaviour in industry such as food and pharmaceutical are essential, since the existence of unwanted bubbles can reduce the quality of product [3]. Tomography method has been introduced to the industrial field and has successfully provided huge contributions in imaging and identifying of the various flow patterns and boundaries. Before the tomography method was introduced, the point sensor was the main type of sensor used in the assessment process. However, the use of a point sensor is not appropriate as it disturb the flow field [4]. Around 1970s, the tomography method was proposed and assimilated in industry for monitoring and designing process [5]. It is termed "Process Tomography" (PT).

The significant advantage of using PT is that the operation can continue without disturbing the process flow since the sensors are located around and outside the pipelines [6]. Hence, the accuracy and efficiency of getting a good product is quite high. For example, the oil and gas industry has applied the method to detect the irregularities in the oil component when the crude oil is transferred from the sea in the pipelines [7]. Another example is in the food technologies industry when the system is used for rice weighing process [8]. The previous research in process tomography focused on measuring several important parameters such as mass flow rate [9], [10], concentration profile [11-13], velocity profile [14] and particles sizing [15]. The sensors that have been used for investigating the two-phase or multiphase flow are ultrasonic, optical, electrodynamics, magnetic induction, electrical resistance and electrical capacitance.

This paper presents an optical tomography system to monitor gas bubbles flow in a vertical pipe using the Independent Component Analysis method. Optical tomography is an attractive method and has a huge potential in the tomography field since it is conceptually straight forward, cheap and has a good dynamic response [16].

2.0 MATHEMATICAL MODELLING

Two parts of mathematical modelling are considered for the system; optical attenuation model and Independent Component Analysis (ICA) model. In the optical attenuation model part, it discusses varying voltage when the gas bubbles were present in the water medium. Whereas, for ICA part, it discusses about the concept of ICA, the application of ICA in various fields and also elaborates several steps for calculating an Average value (Q).

2.1 Optical Attenuation

In this optical attenuation model, the Beer-Lambert's law is applied for modelling the presence of gas bubbles in the liquid medium [17-18]. In this paper, we investigated the level of light energy when it passed through the liquid medium. The energy of light transmitted from a transmitter is attenuated when it reached the receiver. The amplitude voltage for switching on the transmitter is 5 Volt (V). The voltage is set by using a PIC Microcontroller. The amplitude of 5 V is detected by the receiver if there are no voltage losses during the light transmitting from transmitter to receiver. However, light from the transmitter has to pass through the pipe first before it travelled to water and then detected by the receiver. In this condition, light is collimated slightly by the pipe surface, hence the light path may be refracted as well scattered as such it may deviate from the actual route. It caused the voltage to decrease before the light cross the water medium. At the end, the receiver voltage is reduced to between 4.5 V until 4.7 V only. The modeling focused on the attenuation effect rather than the scattering effect since the mathematical modelling for light scattering effect is negligible.The Beer-Lambert's Law can be expressed as:

$$V_R = V_T e^{-\alpha_w L_w - \alpha_g L_g - \alpha_p L_p} \tag{1}$$

$$V_R = V_T e^{-\alpha_t L_t} \tag{2}$$

Where:

V_R = Receiver voltage (V)
V_T = Transmitter voltage (V)
α_w = Attenuation coefficient for water medium (mm^{-1})
L_w = Path length of light travelling through the liquid (mm)
α_g = Attenuation coefficient for gas (mm^{-1})
L_g = Path length of light travelling through the gas (mm)
α_p = Attenuation coefficient for pipe (mm^{-1})
L_p = Path length of light travelling through the pipe (mm)
α_t = Total attenuation coefficient (mm^{-1})
L_t = Total path length (mm)

The transmitter voltage was set at 4.5 V rather than 5 V since the transmitter light experienced voltage losses when it passes through the pipe surface. The attenuation coefficient for water is $\alpha_w = 0.0287$ mm^{-1} and the attenuation coefficient for gas is $\alpha_g = 0.0142$ mm^{-1} [19]. The attenuation coefficient for acrylic pipe is assumed to $\alpha_p = 0.0413$ mm^{-1}. The path length of light travelling through the liquid and pipe is $L_w = 96$ millimetre (mm) and $L_p = 2$ mm respectively. The value of 96 mm is obtained by subtracting 4 mm which represents the pipe surface diameter from the total diameter of the pipe which is 100 mm. Three models of optical attenuation are discussed; no gas bubble, a single gas bubble and double gas bubble in water. Figure 1 shows the light path from a transmitter to a receiver when no gas bubble is present in the water medium. In this case, the energy of light is attenuated water only and L_g is equal to 0 mm. The value of V_R is obtained by:

$$V_R = 4.5 e^{-(0.0287)(96) - 0 - (0.0413)(2)} V \tag{3}$$

$$V_R = 4.5(0.0586) V \tag{4}$$

$$V_R = 0.2635 V \tag{5}$$

The value of 0.0586 in Equation (4) is the total exponential value $(e^{-\alpha_t L_t})$ which is a significant value to investigate for monitoring the presence of gas bubbles using the Independent Component Analysis algorithm. Figure 2 shows a single gas bubble in water medium which interrupts light from transmitter to a receiver.
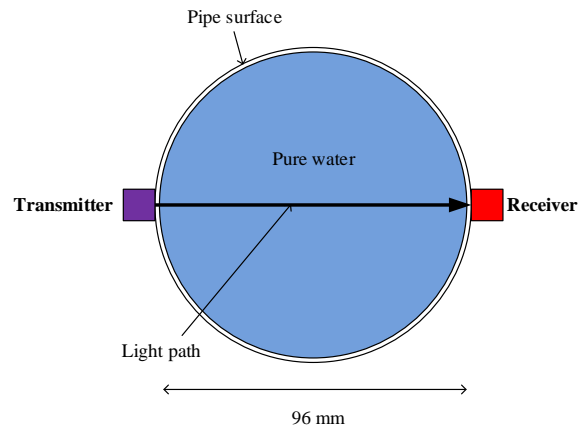
Figure 1 The light path in water when there is no gas bubble in water
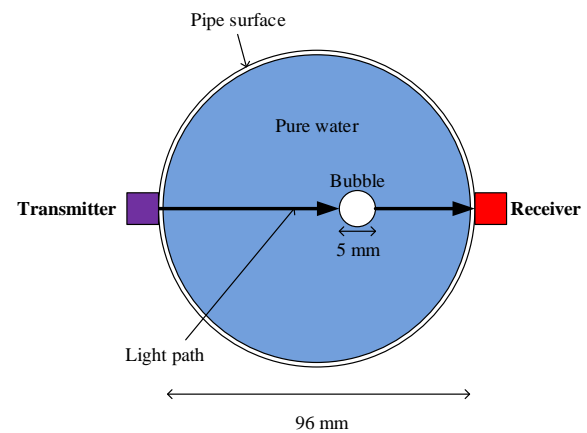
Figure 2 The condition of light path in water when a gas bubble is present in pure water

The value of the receiving voltage, V_R when light passed through the bubble in water can be determined as follows:

$$V_R = 4.5 e^{-(0.0287)(96-5) - (0.0142)(5) - (0.0413)(2)} V \tag{6}$$

$$V_R = 4.5(0.0630) V \tag{7}$$

$$V_R = 0.2833 V \tag{8}$$

For a single bubble flow, the bubble's diameter is $L_g = 5$ mm. The value of total exponential value $(e^{-\alpha_t L_t})$ in Equation (7) is higher when there is a gas bubble flow. This is due to an increase in the attenuation level of energy since the light path has to pass two different medium which are water and gas. Hence, the V_R value also increased. The modelling for double bubble is illustrated as Figure 3. The model represents two different bubble sizes which were generated in the experiment. The equation of the receiving voltage, V_R for double bubbles model is obtained by:

$$V_R = 4.5 e^{-(0.0287)(96-13) - (0.0142)(5) - (0.0142)(8) - (0.0413)(2)} V \tag{9}$$

$$V_R = 4.5(0.0707) V \tag{10}$$

$$V_R = 0.3182 V \tag{11}$$
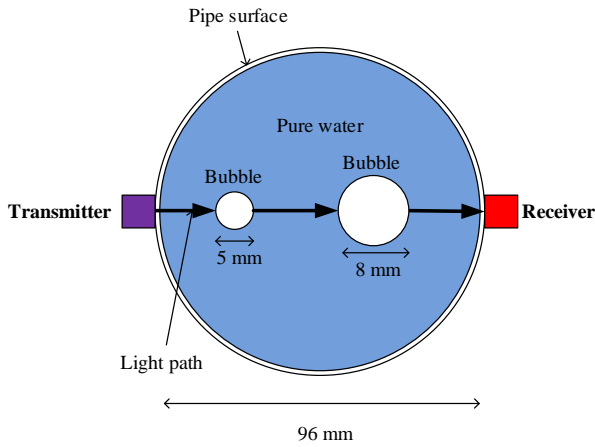
Figure 3 The light path when double bubbles model is present in water

In this case, light has to pass through water and two gas bubbles of different sizes before it reached the receiver. The diameter of the small bubble is L_{g1} = 5 mm and the larger bubble is L_{g2} = 8 mm. The total exponential value for this case is the highest compared to the two previous cases. The presence of several gas bubbles resulted in the attenuation of light. Besides, the value also indicates that the size of gas bubbles plays an important role in determining the value of V_R.

2.1 Independent Component Analysis Model

Independent Component Analysis (ICA) is an attractive method that can solve the Blind Source Separation (BSS). BSS is the problem where information regarding the number of mixed signals is limited, and we do not know how the signals are formed [20]. The problem make it difficult to separate and estimate the process of original source since the specific knowledge about the sources is inadequate [21]. Hence, it is vital to design an adaptive system to solve this problem. ICA has been applied for extracting telecommunication signals [22] and phase flow separation in tomography [21]. It also can be implemented in food technology where Chen and Wang [23] used ICA for estimating the fat content in a meat. Moreover, ICA has been utilized by Polder *et al*. [24] to investigate the spectral images for tomatoes. In another field, Pu and Yang [25] successfully used ICA for classifying the text document based on the topic in a book. In their research, four topics have been selected from a book. Then, using ICA, the text regarding each topic was successfully divided. The general model of ICA is described as:

$$X = AS \qquad (12)$$

where A is an unknown matrix called the mixing matrix. X is the observed signals and S is the source signals. The aim of ICA is to get the mixing matrix (A) and/or source signal matrix (S) given only realizations of the observation matrix of X. The estimation process continued for the sources by obtaining the "unmixing matrix" W, and theoretically $W = A^{-1}$. This enables an estimation of the independent sources to be obtained as:

$$\hat{S} = WX \qquad (13)$$

This research focused on extracting signals at receivers where the signals are transmitted by transmitters surrounding the pipe. The illustration for this case is shown in Figure 4. In Figure 4, two signal transmitters which have different pulse durations are

transmitted to two receivers. Using ICA, both signals are separated and brought along the separating matrix ($\hat{S}$) in an arbitrary form. The mathematical model for an application of ICA for two pairs of sensors and two attenuation coefficients is shown in Figure 5.

In Figure 5, TX1 and TX2 indicate transmitter 1 and transmitter 2 respectively while RX1 and RX2 are receiver 1 and receiver 2 respectively. Two attenuation coefficients are denoted as α_1 and α_2.
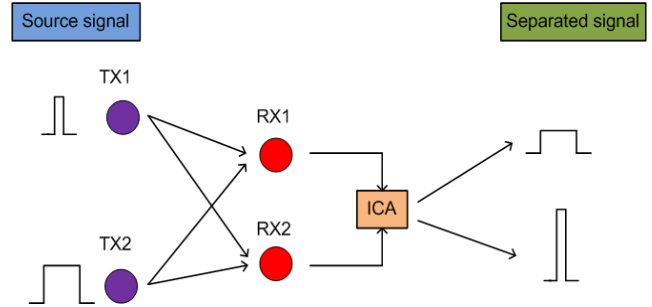
Figure 4 The illustration of applying the ICA concept in transmitters and receivers
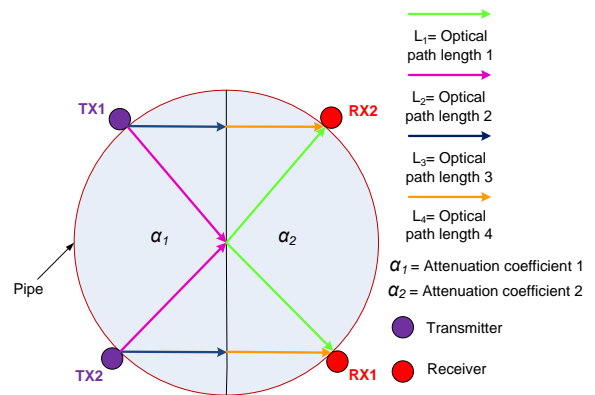
Figure 5 Model of two sensor's pair with two attenuation coefficients

In this case, each receiver has detected the signals from both transmitters. The equation for the voltage at receiver 1 (V_{R1}) and voltage at receiver 2 (V_{R2}) are written as:

$$V_{R1} = V_{T1}e^{-\alpha_1 L_2} + V_{T1}e^{-\alpha_2 L_4} + V_{T2}e^{-\alpha_1 L_3} + V_{T2}e^{-\alpha_2 L_4} \qquad (14)$$

$$V_{R2} = V_{T1}e^{-\alpha_1 L_3} + V_{T1}e^{-\alpha_2 L_4} + V_{T2}e^{-\alpha_1 L_2} + V_{T2}e^{-\alpha_2 L_1} \qquad (15)$$

Equations (14) and (15) are simplified as follows:

$$V_{R1} = V_{T1}e^{-\alpha_1 L_2 - \alpha_2 L_1} + V_{T2}e^{-\alpha_1 L_3 - \alpha_2 L_4} \qquad (16)$$

$$V_{R2} = V_{T1}e^{-\alpha_1 L_3 - \alpha_2 L_4} + V_{T2}e^{-\alpha_1 L_2 - \alpha_2 L_1} \qquad (17)$$

Equations (16) and (17) can be written in the matrix form as follows:

$$X = A \quad S$$

$$\begin{bmatrix} V_{R1} \\ V_{R2} \end{bmatrix} = \begin{bmatrix} e^{-\alpha_1 L_2 - \alpha_2 L_1} & e^{-\alpha_1 L_3 - \alpha_2 L_4} \\ e^{-\alpha_1 L_3 - \alpha_2 L_4} & e^{-\alpha_1 L_2 - \alpha_2 L_1} \end{bmatrix} \begin{bmatrix} V_{T1} \\ V_{T2} \end{bmatrix} \quad (18)$$

where V_{R1} and V_{R2} represent the observed signal (X), $e^{-\alpha_t L_t}$ is the mixing matrix (A) whereas V_{T1} and V_{T2} represent the source signals (S). The parameter of interest in Equation (18) is the matrix A. Based on the mathematical modelling in the optical attenuation model, $e^{-\alpha_t L_t}$ is varied when gas bubbles interrupted the light transmitting path. The output matrix after the implementation of the ICA algorithm is written as equation (19). Matrix A can be obtained by inversing the matrix W since theoretically in ICA, $W = A^{-1}$.

$$\hat{S} = W \quad X$$

$$\begin{bmatrix} V_{R1} \\ V_{R2} \end{bmatrix} = \begin{bmatrix} W_{1,1} & W_{1,2} \\ W_{2,1} & W_{2,2} \end{bmatrix} \begin{bmatrix} V_{T1} \\ V_{T2} \end{bmatrix} \quad (19)$$

Practically, the measurement system consists of eighteen transmitters and eighteen receivers. Hence the equation for the output matrix can be written as:

$$\hat{S} = W \quad X$$

$$\begin{bmatrix} V_{R1} \\ \vdots \\ V_{R18} \end{bmatrix} = \begin{bmatrix} W_{1,1} & \cdots & W_{1,18} \\ \vdots & \ddots & \vdots \\ W_{18,1} & \cdots & W_{18,18} \end{bmatrix} \begin{bmatrix} V_{T1} \\ \vdots \\ V_{T18} \end{bmatrix} \quad (20)$$

The calculation for getting the Average value (Q) is based on the following steps:

a) ICA is used for separating the eighteen signals from the sensors into a single transmitter signal. ICA produced an unmixed matrix (W) which is in an arbitrary row. Matrix W has to be rearranged as written in Equation (20) based on the transmitter's pulse duration. Transmitter 1 (TX1) is set to 1 millisecond (ms), transmitter 2 (TX2) is set to 2 ms and followed until transmitter 18 (TX18) which is set to 18 ms respectively.

b) In the ICA theory, $W = A^{-1}$. The matrix A which is also known as the turbidity factor is the parameter of interest. Mixing matrix (A) is indicated as $e^{-\alpha_t L_t}$ which has 18 columns and 18 rows. It represents the 18 receivers and 18 transmitters respectively. The matrix of A can be written as $A_{j,k}$ where j is the transmitter number and k is the receiver number.

c) As an example, let the value of $A_{3,2}$ as 1.632. This indicates that, the light transmitted from transmitter TX3 to receiver RX2 have a turbidity factor of 1.632.

d) Pixels (Z) is the affiliation between A and light's path length, where light crossed a pixel. The Z value is calculated by:

$$Z_{r,c} = (u/t) \times A_{j,k} \quad (21)$$

where r and c represents the row and column respectively. u is the path length of light that pass through the pixel in cm and t is the total length from the transmitter to the receiver. For example, in the case of light from transmitter TX3 to receiver RX2, matrix A resulted in $A_{3,2} = 1.632$. Figure 6

represents the circular pipe when it is imposed on a sensitivity map. In Figure 6, u for Pixel {2,15} is 0.5 cm and the total light path length from transmitter 3 to receiver 2 is $t = 1$ cm. Hence, Pixel {2,15} can be calculated by using equation (21):

$$Z_{2,15} = (0.5 \text{ cm}/1 \text{ cm}) \times 1.632 \quad (22)$$
$$Z_{2,15} = 0.816 \quad (23)$$

e) Pixel {2,15} is intercepted by 3 light paths coming from transmitters TX3,TX4 and TX5. Then, the value of Z is recalculated again based on the light's path length and A value. The process is expanded to receivers RX2 until RX18. Lastly, the P value from all transmitters is totalled up and divided back with how many number of light path length that have crossed the pixel in order to get the Average value (Q). The Q value will be used to analyse and monitor the gas bubble behavior in the pipe.
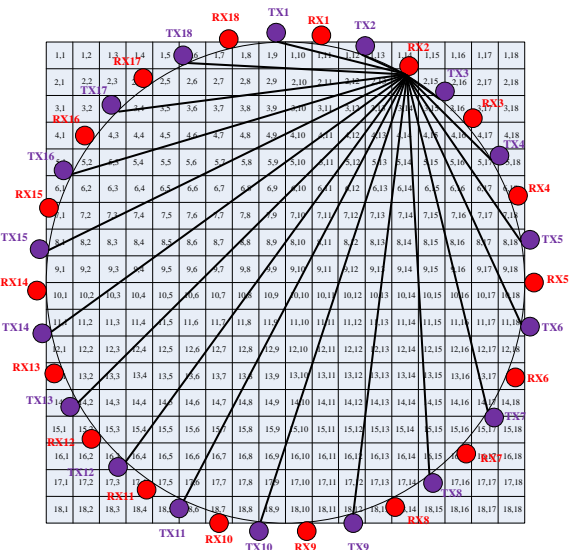
Figure 6 Transmission of light towards receiver 2

■3.0 THE MEASUREMENT SYSTEM

This section elaborates the hardware and software design. The hardware part consists of the design of pipe, sensor jig and signal conditions circuits. This part also introduced the use of Data-Acquisition System (DAS) in assisting the capture of data from the sensors and reconstruction of images. For software design, the discussion covers on the LabVIEW software, the synchronisation system and the implementation of ICA.

3.1 Hardware Design

The system consists of a transparent vertical pipe made from acrylic material and it has a diameter of 100 mm. Eighteen pairs of transmitters and receivers are installed around the pipe using a sensor jig. The infrared transmission light is selected in order to ensure that the receivers have detected light from the transmitters only, and not the light from surrounding such as a laboratory lamp. This characteristic of light is essential in order to obtain a good and accurate analysis. The signal conditioning circuit is designed to amplify the signal received from the transmitter. The input received by photodiode model BPV10NF is in physical signal form, which is represented by light. The BPV10NF photodiode is selected since it has a peak wavelength (λ_p) of 940 nm which is the same as the peak wavelengths value of the transmitter. It is important for both transmitter and receiver to

have equal or near the peak wavelength of each other in order to detect the infrared light.

The BPV10NF model has ±20° angle of half sensitivity and 2.5 ns of rise time. The data-acquisition system (DAS) model U2331 manufactured by Agilent Technologies is used for capturing and analysing the data. The image reconstruction of the bubble flow is displayed using a computer. Figure 7 shows the overall design of the optical tomography system. The air flow is injected from the bottom of the vertical pipe and rises upwards. The quantity of bubble flow is varied by altering the valve in order to get a 25%, 50% and 100% of air opening. Other than that, the experiment using a single bubble flow and double bubble's flow is done for verifying the precision and accuracy of the system using the ICA algorithm. The result of the experiment demonstrates that the system can detect the existence of gas bubble in pure water. Five experiments have been carried out which are a single bubble flow, double bubble flow, 25% of air opening, 50% of air opening and 100% of air opening. The Q value for each experiment is recorded and analysed. The Q value is converted to concentration profile using the LabVIEW software.

3.2 Software Design

The LabVIEW software manufactured by National Instrument (NI) which is based on graphical system design was utilized in this project. LabVIEW has two components for interfacing, which are in the form of a block diagram and a front panel. The block diagram contains the graphical source code for the developed work such as in mathematical, analysis, testing and control process. Besides, the front panel is the section where the graphical user interface (GUI) is created and the outcome is displayed. The software provides the easiest way to construct the GUI for analysis by containing many tools for data visualisation such as graph, chart, matrix indicator and digital waveform.
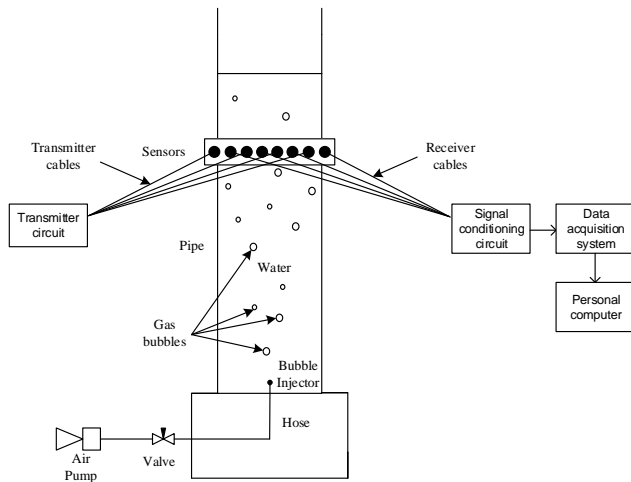
Figure 7 An optical tomography system

The other advantage of using LabVIEW is that it has the capability to synchronise with the hardware or software from other companies such as Agilent Technologies, Mathworks and Texas Instruments (TI). The connection of the block diagram for synchronisation process between DAS and LabVIEW is shown in Figure 8. Eighteen block diagrams for analog input are utilized in the LabVIEW since the optical system consists of eighteen receivers. The range for the input voltage is from 0 Volt (V) until 10 V and the sampling rate is set to 1000 Hz.
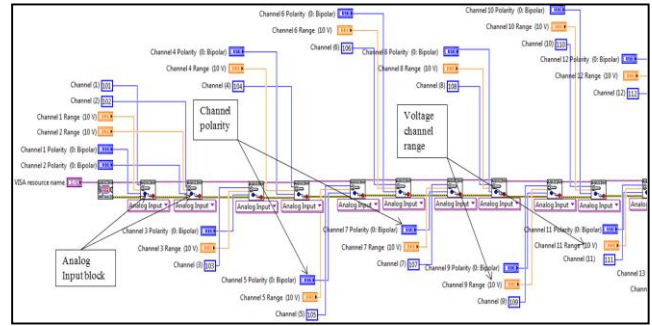
Figure 8 The block diagram for synchronisation process for DAQ and LabVIEW software

■4.0 RESULT AND DISCUSSION

Q value is obtained from the calculation as discussed in previous section. Q value is the pixel value which then converted to concentration profile in order to get easier for indicating the difference of colour for each pixel in the pipe. The gas bubble flow condition and the result of concentration profile are shown in Table 1. For all experiments, the result of Q value indicates that the location of gas bubble can be estimated by looking at the higher value of the pixel. The presence of gas bubble has increased the value of Q as discussed in the mathematical modelling section. The location of bubble is shown in pink colour, which has the highest Q value compared to other pixels. The concentration profile for a single bubble flow and double bubble flow shows that the pink colour is located near the pipe's border rather than middle of the pipe. The pixel concentration at the pipe's border is higher compared to other pixels due to the installation of the receivers around the pipe. Most of the lights have a tendency to cross the pixels which are located near the pipe surface. Although the average value has been taken, the pixels' value near that location is still high compared to other locations. For experiments involving 25%, 50% and 100% of air opening, the Q values are also high at the border of pipe. This is because, some bubbles are inclined to rise towards the pipe's border, although the air flow is injected at the centre of the pipe base.

■5.0 CONCLUSION

An optical tomography system has been developed for imaging the gas bubble behaviour in pipe using ICA algorithm. The imaging process has been performed without interrupting the process flow since the optical sensors are mounted outside the pipe. An optical attenuation model is described for obtaining the voltage properties between water and air. The Q value is obtained based on the ICA algorithm and the concentration profile for the gas bubbles flow is reconstructed. The concentration profile for the gas bubble flow has been reconstructed using the LabVIEW software and the optical sensors are sensitive to the variation of the gas bubbles flow which are single bubble, double bubble, 25% of air opening, 50% of air opening and 100% of air opening. The presence of gas bubbles at pixels contain in the pipe has increased the Q value. Therefore, we can estimate the location and quantity of gas bubbles enclose in the pipe. The system has provided sufficient information and has the potential to be applied in the process industry for increasing the optimisation of the process. However, the system has a limitation which needs to overcome.

The use of filter method for concentration profile is vital especially for filtering the high Q value near to the pipe's border which can provide better visual for gas bubbles.

Table 1 The gas bubble condition and concentration profile

Gas bubble flow	Gas bubble condition	Concentration profile
A single bubble		
Double bubble		
25% of air opening		
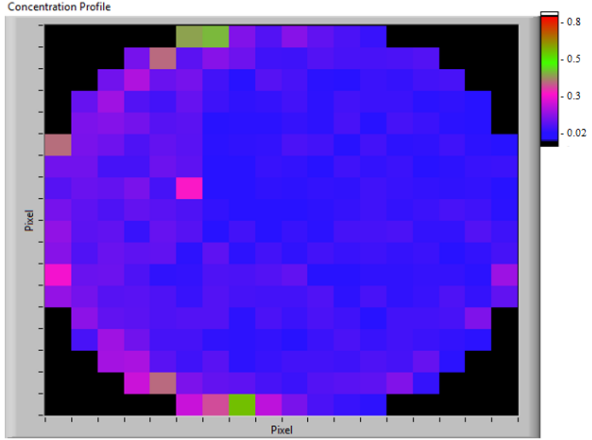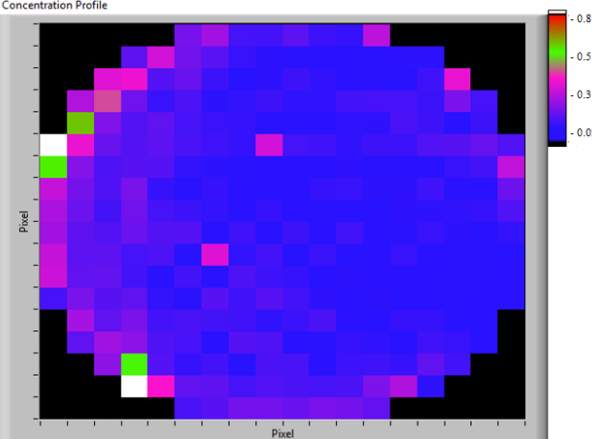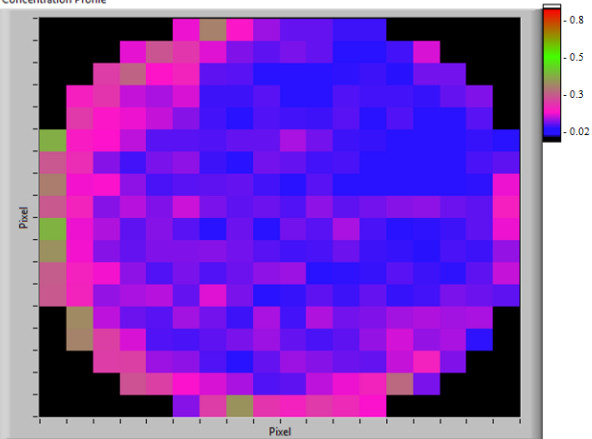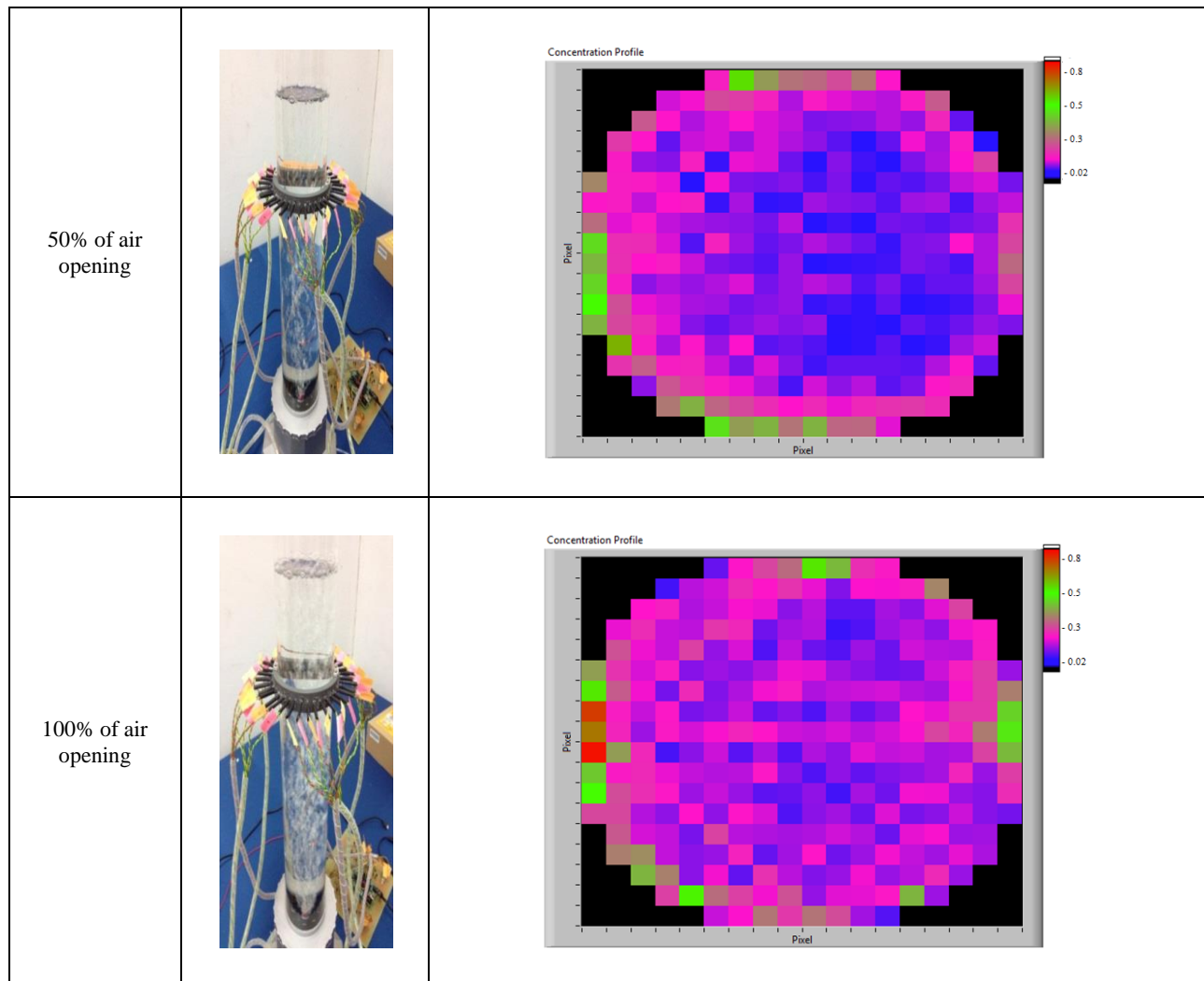
50% of air opening		
100% of air opening		

References

[1] Dyakowski, T. 1996. Process Tomography Applied to Multi-Phase Flow Measurement. *Measurement Science and Technology*. 7: 343–353.

[2] Schleicher, E., Silva, M. J., Thiele, S., Li, A., Wollrab, E., and Hampel, U. 2008. Design of an Optical Tomograph for the Investigation of Single- and Two-Phase Pipe. *Measurement Science and Technology*. 19: 1–14.

[3] Detsch, R. M., and Sharma, R. N. 2000. The Critical Angle for Gas Bubble Entrainment by Plunging Liquid Jets. *The Chemical Engineering Journal*. 44(1990): 157–166.

[4] Ibrahim, S., Yunus, M. A. M., Green, R. G., and Dutton, K. 2012. Concentration Measurements of Bubbles in a Water Column using an Optical Tomography System. *ISA Transactions*. 51(6): 821–826.

[5] Beck, M. S., and Williams, R. A. 1996. Process Tomography: A European Innovation and its Applications. *Measurement Science and Technology*. 7: 215–224.

[6] Zhao, Y., Hu, S., and Wang, Q. 2013. Research Progress of the Optical Fiber Sensors in Process Tomography. *Instrumentation Science & Technology*. 41: 154–174.

[7] I. Ismail, J. C. Gamio, S. F. A. Bukhari, and W. Q. Yang. 2005. Tomography for Multi-phase Flow Measurement in the Oil Industry. *Flow Measurement and Instrumentation*. 16:145–155.

[8] Mohd Muji, S. Z. 2012. *Optical Tomography for Solid Gas Measurement using Mixed Projection*. PhD Thesis, Universiti Teknologi Malaysia, Skudai.

[9] Zheng, Y., and Liu, Q. 2011. Review of Techniques for the Mass Flow Rate Measurement of Pneumatically Conveyed Solids. *Measurement*, 44(4): 589–604.

[10] Hunt, A. 2014. Weighing without Touching: Applying Electrical Capacitance Tomography to Mass Flowrate Measurement in Multiphase Flows. *Measurement and Control*. 47(1): 19–25.

[11] Thuku, I. T., Rahmat, M. F., Wahab, N. A., Tajdari, T., and Yusuf, A. A. 2013. 2D Finite Element Modeling of Electrostatic Sensor for Tomography System. *Sensor Review*. 33(2): 104–113.

[12] Ibrahim, S., Yunos, Y. M., Green, R. G., and Dutton, K. 2001. A Tomography System Using Optical-Fibre Sensors for Measuring Concentration and Velocity of Bubbles. *Measurement and Control*. 34(2): 47–51.

[13] Mingsheng, W., Minming, T., Jifei, H., Li, C., and Jie, X. 2012. Detection of Coal Dust in a Mine using Optical Tomography. *International Journal of Mining Science and Technology*. 22: 523–527.

[14] Tan, C., and Dong, F. 2010. Cross Correlation Velocity of Oil-water Two-Phase Flow by a Dual-Plane Electrical Resistance Tomography System. In *Instrumentation and Measurement Technology Conference (I2MTC)*. 766–770.

[15] Idroas, M., Abdul Rahim, R., Fazalul Rahiman, M. H., Ibrahim, M. N., and Green, R. G. 2011. Design and Development of a CCD Based Optical Tomography Measuring System for Particle Sizing Identification. *Measurement*. 44(6): 1096–1107.

[16] Ibrahim, S., Green, R. G., Dutton, K., Evans, K., Rahim, R. A., and Goude, A. 1999. Optical Sensor Configurations for Process Tomography. *Measurement Science and Technology*, 10: 1079–1086.

[17] R. Abdul Rahim, Y. Md. Yunos, M. H. Fazalul Rahiman, and H. Abdul Rahim, 2010. Mathematical Modelling of Gas Bubbles and Oil Droplets in Liquid Media using Optical Linear Path Projection. *Flow Measurement Instrumentation.*, 21(3): 388–393.

[18] S. Ibrahim, 2000. *Measurement of Gas Bubbles in a Vertical Water Column using Optical Tomography*. PhD Thesis, Sheffield Hallam University, United Kingdom.

[19] Daniels, A. R. 1996. *Dual Modality Tomography for the Monitoring of Constituent Volumes in Multi-Component Flows*. PhD Thesis, Sheffield Hallam University.

[20] Naik, G. R., and Kumar, D. K. 2011. An Overview of Independent Component Analysis and Its Applications. *Informatica*. 35: 63–81.

[21] Xu, Y., Wang, H., Cui, Z., Dong, F., and Yan, Y. 2010. Separation of Gas-Liquid Two-Phase Flow Through Independent Component Analysis. *IEEE Instrumentation And Measurement*. 59(5): 1294–1302.

[22] Huang, J. P., and Mar, J. 2004. Combined Ica and Fca Schemes for Hierarchical Network. *Wireless Personal Communications*. 28(1): 35–58.

[23] Chen, J., and Wang, X. Z. 2001. A New Approach to Near-Infrared Spectral Data Analysis using Independent Component Analysis. *Journal of Chemical Information and Computer Sciences*. 41: 992–1001.

[24] Polder, G., Heijden, G. W. A. M. Van Der, and Young, I. T. 2003. Tomato Sorting using Independent Component Analysis on Spectral Images. *Real-Time Imaging*. 9(9): 253–259.

[25] Pu, Q., and Yang, G. 2006. Short-Text Classification based on ICA and LSA. *Advance in Neural Network-ISNN 2006*. 3972: 265–270.